TORSIONAL MEMS SCANNER BASED ON $LiNbO_3$ THIN FILM

Yushuai Liu[1,2,3]*, Zhiyuan Gao*[1]*, Kangfu Liu*[1,2,3]*and Tao Wu*[1*]
[1]School of Information Science and Technology, ShanghaiTech University, CHINA
[2]Shanghai Institute of Microsystem and Information Technology,
Chinese Academy of Sciences, CHINA
[3]University of Chinese Academy of Sciences, CHINA

ABSTRACT

This article presents the micro-scanners based on 36Y-cut lithium niobate thin film ($LiNbO_3$) to be used for projection display and optical attenuators. Through the analysis of different design parameters of micro-scanner structure, $LiNbO_3$ micro-scanner has been proved to have lithographically defined scanning frequency with large scanning angles. A micro-scanner of high scanning angle has been designed, fabricated and characterized. The design has a total size of 15×270 μ m^2, and driving efficiency of 13.21° at 135.5 kHz and input voltage of 10 V. Our devices show great potential for micro-scanners application where it has large potential of raster scanning upon further scaling in driving efficiency.

KEYWORDS

Micro-scanner, $LiNbO_3$ thin film, high scanning angle, high frequency

INTRODUCTION

Microelectromechanical systems (MEMS) technology enables the building of micro-scanners that are well suited for small size, low cost and scalability [1]. The scanner resolution is determined by the mirror dimension (*D*), the optical beam deflection angle θ_{opt}, and the scanning frequency f [2]. The optical beam deflection angle θ_{opt} discussed in this article is equivalent to 4 θ_{mech} for laser light incident diagonally on the scanning mirror in the direction of deflection, as determined from trigonometry [3]. Electrostatic, electromagnetic and piezoelectric scanners all can be used as the driving mechanisms of the scanning mirror. Among them, piezoelectric scanners are mainly used for low driving voltage, high scanning force and smaller size. Piezoelectric MEMS scanners can also excite resonant frequency of the torsional mode to achieve the scanning devices of both high speeds and wide angles [4]. Therefore, it has become the main driving mechanisms for micro-scanners.

Piezoelectric actuation with thin-film PZT is a promising piezoelectric material due to its potential to offer equal performance at much lower voltage levels than electromagnetic scanners and its much smaller package size, compared with electromagnetic scanners [1]. For example, thick PZT with stainless steel substrate was used to resonate at 28 kHz with 1 mm mirror aperture and achieved a 41° optical angle [5]. A PZT micro-scanner is reported in achieving 23°·mm at 4.3 kHz and 104°·mm at 90.3 Hz [6]. Other published approaches use thin/thick PZT on different types of substrates such as Pt-coated Ti substrates and it can also be grown on other substrates such as Si or MgO [7, 8]. Although the PZT scanner is a promising candidate to meet the requirements of both relatively low voltage and high driving scanning angle. Mechanical design challenges of damping losses at resonant frequency and limited deflection of PZT beams with large stiffness still remain to be solved [1]. In addition, the piezoelectric coefficients d_{31} determines that PZT scanners is mainly excited by 3-direction electric field and the upper and bottom electrode structure must be constructed.

As a new piezoelectric material, single crystal $LiNbO_3$ films has become available as a piezoelectric material via film transfer techniques [9]. In contrast to PZT, it provides smoother surface and larger deflection. And it also demonstrates the large piezoelectric coefficients of d_{16} in the 36Y-cut, which means that it only replied on the upper electrodes which can achieve the micro-scanners. It greatly simplifies the fabricated process. However, micro-scanners based on $LiNbO_3$ film have not been extensively explored. In this paper, we have developed a MEMS micro-scanner composed of piezoelectric $LiNbO_3$ film on the Si substrate. We demonstrate the simulation analysis and fabricated devices of direct-driving single-axis scanning mirror using $LiNbO_3$ piezoelectric scanner where the force/torque is directly applied on the scanning mirror frame [10]. We have analyzed the driving efficiency of $LiNbO_3$ micro-scanners under different design parameters, and demonstrated the fabricated micro-scanners with high angular drive efficiency, low power consumption (1-10V), and a simple fabrication process.

DESIGN AND ANALYSIS

Micro-Scanner Structure

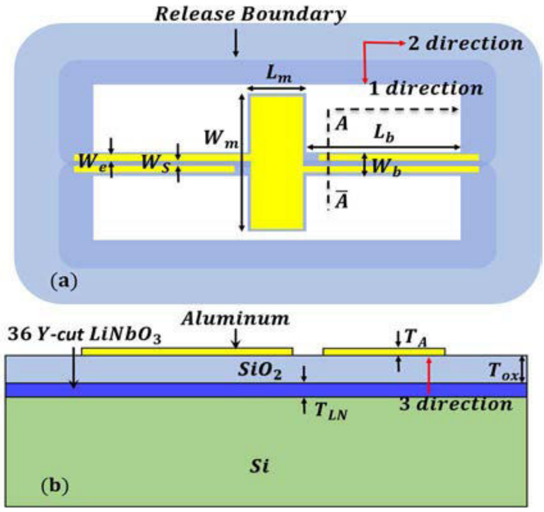

Figure 1. (a) Top view and (b) Cross section view of the micro-scanner

As shown in Fig. 1, the micro-scanner structure consists of a $LiNbO_3$ layer (0.7 μm) and a silicon oxide (SiO_2) layer. The SiO_2 layer on the top of $LiNbO_3$ layer acted as the bending layer. From the top view, the scanner needs to be tethered via two actuators. Every actuator with a pair of interdigitated electrodes can cause in-plane shear stress around the out-of-plane when the electric field is applied along the x-direction. The two actuators are driven with voltage of opposite polarities to make them work in tandem.

$LiNbO_3$ Orientation Selection

As we know, $LiNbO_3$ is an anisotropic crystal with different material properties in different cut orientations. To maximize the scanning efficiency of our $LiNbO_3$ micro-scanner, the orientation (crystal cut) and the direction of the applied electric field have to be carefully selected for the desired mode of operation. 36Y-cut $LiNbO_3$ rotated e-matrix is shown as below:

$$e = \begin{bmatrix} 0 & 0 & 0 & 0 & 0.1 & -4.5 \\ -1.7 & -2.3 & 2.6 & 0.5 & 0 & 0 \\ -1.94 & -1.6 & 4.5 & -0.3 & 0 & 0 \end{bmatrix} C/m^2 \quad (1)$$

As shown in Equ. (1), the 36Y-cut $LiNbO_3$ has a large piezoelectric stress constant component of -4.5 (C/m^2) in e_{16} [4], which can excite the torsional mode vibration with top-only interdigitated transducers (IDT). The orientation is identified as the X-axis of $LiNbO_3$ crystal, along which the electrical field will be applied to fully harness the e_{16} for maximum scanning efficiency. By default, (δ, β, γ) are used to represent the Euler rotation angle; therefore for 36Y-cut $LiNbO_3$, the Euler rotation angle is (δ, 54, 0). The electrode arrangement direction is along the x-axis direction, and δ represents the direction of wave propagation.

Structure Parameters Analysis and Design

The resonant frequency (f) of the micro-scanner shown in Fig. 1 can been expressed as follows [3, 4]:

$$\mathrm{f} = (1/2\pi)\sqrt{2J_b G/L_b J_m} \quad (2)$$

where J_m is the mirror moment of inertia, J_b is the torsional constant, G is the shear modulus. J_b can be expressed as follows:

$$J_b = W_b T^3 (\tfrac{1}{3} - 0.21\tfrac{T}{W_b}(1 - \tfrac{T^4}{12{W_b}^4}) \quad (3)$$

where T is the total thickness of $LiNbO_3$ film (T_{LN}) and SiO_2 (T_{ox}). J_m can been formulated as follows:

$$\mathrm{J}_m = \rho \mathrm{T} L_m {W_m}^3/12 \quad (4)$$

where ρ is the material density. As shown in the cross-section view of Fig. 1 (b), we firstly deposit SiO_2 on the $LiNbO_3$ film, which provides a lot of convenience for the design and fabrication process of the micro-scanner. SiO_2 layer is critical for enhancing the response of $LiNbO_3$ micro-scanner. The thickness of SiO_2 layer can have effect on the frequency and displacement of micro-scanner according to Equ (2) and Fig. 2 (a). It offers an idea of adjusting the working frequency and displacement of the micro-scanner by adjusting the thickness of SiO_2 layer.

Different from the single MEMS resonator, micro-scanner consists of a rotated mirror plate and two scanners. Therefore, there are many parameters that can affect the performance of the micro-scanner. As is shown in Fig. 2, we analyzed the influence of different parameters on the displacement of micro-scanner through COMSOL simulation. The displacement represents the distance of rotated mirror plate along the 3-direction shown in Fig. 1 (b). When the oxide-to-$LiNbO_3$ thickness ratio $\alpha = 0.3$, i.e. the thickness of SiO_2 is 210 nm, a max displacement can be achieved at a typical design space L_m = 15 μm, W_m = 70 μm, L_b = 100 μm and W_b = 8 μm.

The scanner displacement has a rapid increasing when electrodes coverage goes from 0.2 to 0.6. And it reaches a max value when electrodes coverage is 0.6. For other four layout design parameters, W_m and L_b are positively correlated with the displacement. It means that the displacement response of the micro-scanner can be adjusted by changing the size of the micro-scanner structure. The scanner displacement has a rapid decreasing when W_b goes from 8 μm to 20 μm. However, L_m has little impact on the scanner torsional rotation and displacement.

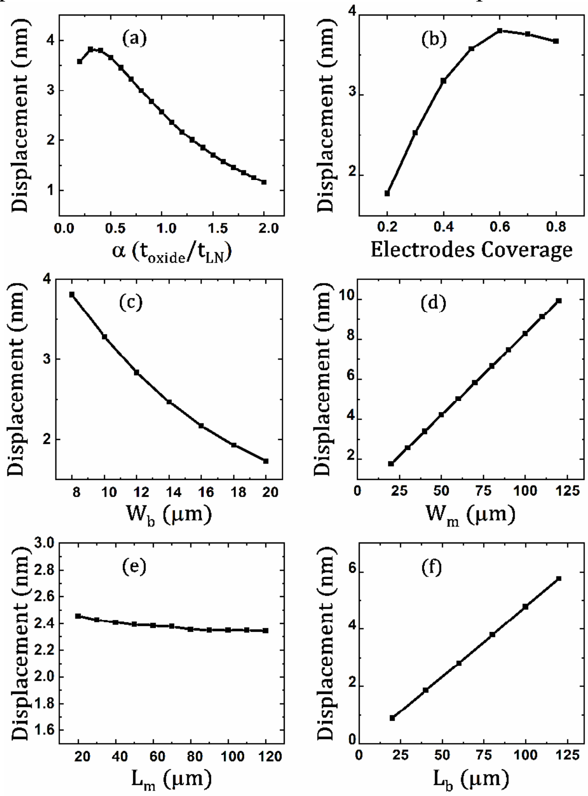

Figure 2. The relations between structure parameters of α, electrodes coverage, W_b, W_m, L_m and L_b and displacement

According to Equ. (2) and our simulation analysis, there are some design trade off between the displacement and frequency. We can achieve high frequency or high deflected displacement. $LiNbO_3$ film based Micro-scanner can achieve lithography defined frequency and driving efficiency, which provides guidance to implement multi-frequency and multi-displacement micro-scanner on the same substrate.

In order to increase the rotated displacement of micro-scanner, the design of large displacement has been demonstrated. The design parameters of large displacement are shown in Table 1. The simulated angular drive efficiency is analyzed in COMSOL (assuming Q=100) and plotted in Fig. 3. The design of large-θ_{mech} has a driving efficiency of 1.68 °/V at 139 kHz shown in Fig. 3. The angular drive efficiency can be defined as θ_{mech} per applied drive voltage. θ_{mech} is the zero-to-peak mechanical angle (marked in Fig. 3).

Table 1 Parameters for the micro-scanner

Parameter	Description	Design[μm]
L_b	Beam length	100
W_b	Beam width	8
L_m	Mirror length	15
W_m	Mirror width	70
W_e	Electrode width	2
W_s	Electrode spacing	2
T_{ox}	SiO_2 thickness	0.21
T_{LN}	$LiNbO_3$ thickness	0.7
T_A	Al thickness	0.2

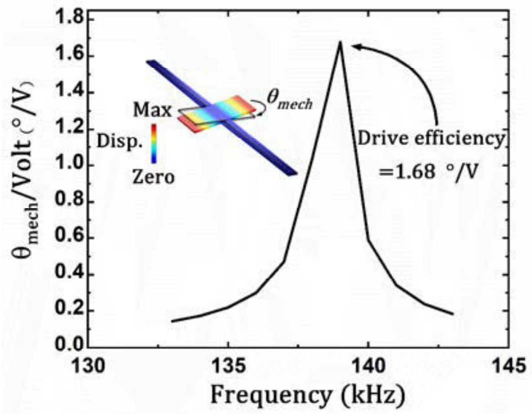

Figure 3. Simulated angular drive efficiency at driving voltage of 1 V and Q of 100

FABRICATION AND MEASUREMENTS

The fabrication process and are shown in Fig. 4 (a) and the microscopic images of fabricated device are shown in Fig. 4 (b). A 36Y-cut $LiNbO_3$ sample starts with transfer-bonding a 36Y-cut $LiNbO_3$ film (0.7 μm) to a silicon carrier (500 μm) using the ion-slicing process. The SiO_2 film is deposited using Plasma-enhanced chemical vapor deposition (PECVD). Before the etching process, a hard baking at 115℃ for 10min is performed for AZ5214 to harden the photoresist (PR) to serve the mask for etching SiO_2 layer and $LiNbO_3$ layer. Next, we use reactive ion etching (RIE) to etch SiO_2 and ion beam etching (IBE) to etch $LiNbO_3$ [11]. Afterwards, the photoresist mask (AZ5214) is removed with Piranha, and 200 nm Al metal is subsequently defined on top of the $LiNbO_3$ film as the IDT electrodes using a lift-off process. Finally, the micro-scanner is released by using XeF_2 isotropic etching to remove the silicon underneath.

The measured θ_{mech} with different design parameters, which can be obtained by Polytec MSA-600, is shown in Fig. 5 (a)-(d). Note that the drive voltage herein is set to 5 V. All rotated mechanical angle under parameters of electrodes cover, L_b, L_m and W_b have the consistent trends with the simulated. The effect of actual W_m can be ignored, so the measured isn't displayed. The θ_{mech} has the highest response when electrode coverage is 0.5. The structural parameters of L_b are positively correlated with θ_{mech} and W_b is negatively correlated with θ_{mech}. It provides a basis for our design of large-θ_{mech} micro-scanner. According to this feature, micro-scanner based $LiNbO_3$ can achieve lithography defined displacement, which provides guidance to implement multi-displacement micro-scanner on the same sample.

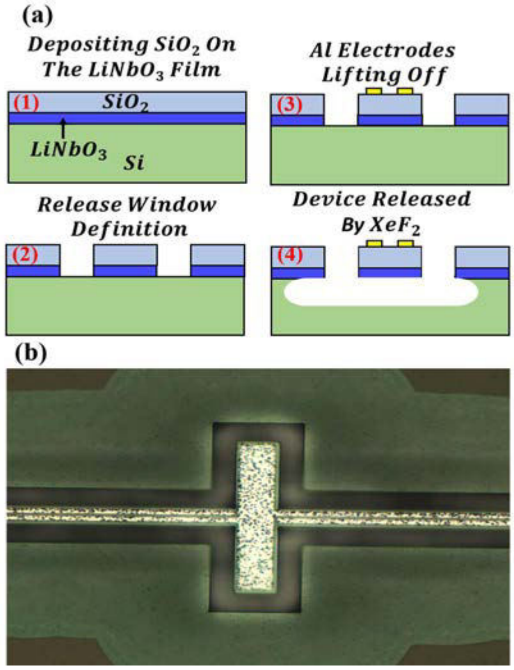

Figure 4. (a) The fabrication process of Micro-scanner; (b) Optical microscope image

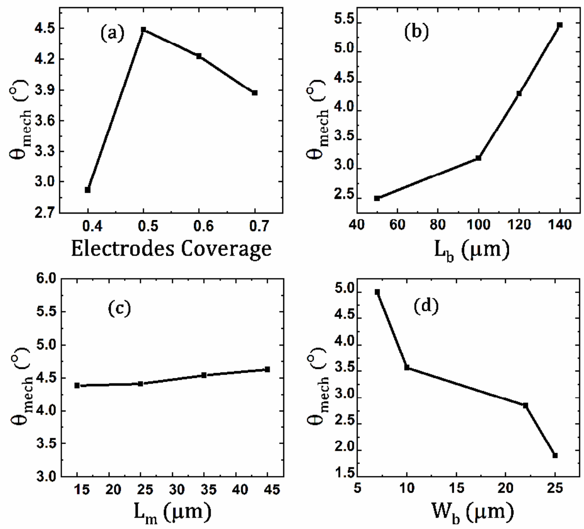

Figure 5. The measured θ_{mech} for different design parameters (a)electrodes coverage, (b)L_b, (c)L_m and (d) W_b at driving voltage of 5V

The design of large-θ_{mech} has also been measured as shown in Fig. 6 (a). The design has the quality factor (Q) of 97 and the driving efficiency is 1.46 °/V at 135.5 kHz in the air shown in Fig. 6 (a). It is close to the simulate angular drive efficiency 1.68 °/V. The low quality comes from the large size of micro-scanner and the rough fabrication. And, high Q can help achieve larger θ_{mech}. The measured mechanical angle (θ_{mech}) of design 1 based different input voltage level are plotted in Fig. 6 (b). The θ_{mec} increases with input voltage increasing and θ_{mec} is 13.21 ° when input voltage is 10 V.

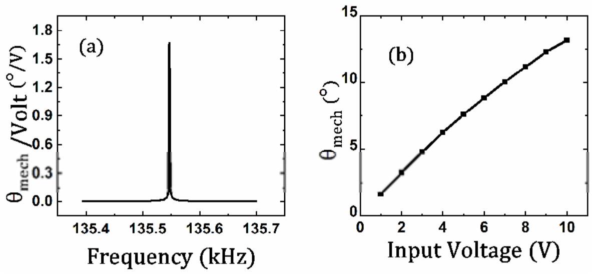

Figure 6. (a) The measured angular drive efficiency (Q=97) and (b) the measured mechanical angle (θ_{mech}) as a function of input voltage

$LiNbO_3$-based micro-scanner is compared with the torsional scanners targeting the raster scanning applications. PZT is widely used in the previous raster scanning applications. Our fabricated device has demonstrated large frequency, low driving voltage and high optical rotating angle.

Table 2 Comparison of different scanners

Ref	θ_{opt} (°)	Voltage (V)	Frequency (kHz)	Size (mm^2)
[2]	54	5	38	1
[13]	22	20	25.4	1
[14]	41	42	25.4	0.5
This Work	52.84	10	136	0.27×0.015

CONCLUSION

The driving efficiency of micro-scanner based on $LiNbO_3$ film was analyzed under different design parameters. $LiNbO_3$ micro-scanner has been proved to have lithographically defined frequency and scanning displacement. Optimized scanning angle θ_{mech} has been designed, fabricated, and measured. The design of large driving θ_{mech} has a mirror size at 15×70 μm^2, which has the driving efficiency of 13.21 ° at 135.5 kHz when input voltage is 10 V. Our design shows great potential of micro-scanners applications where it needs high scanning angle and scalable frequency.

REFERENCES

[1] U. Baran *et al.*, "Resonant PZT MEMS scanner for high-resolution displays," *Journal of microelectromechanical systems,* vol. 21, no. 6, pp. 1303-1310, 2012.

[2] T. Iseki, M. Okumura, and T. Sugawara, "High - Speed and Wide - Angle Deflection Optical MEMS Scanner Using Piezoelectric Actuation," *IEEJ Transactions on Electrical and Electronic Engineering,* vol. 5, no. 3, pp. 361-368, 2010.

[3] H. Urey, "Torsional MEMS scanner design for high-resolution scanning display systems," *Proceedings of SPIE - The International Society for Optical Engineering,* vol. 4773, pp. 27-37, 2002.

[4] A. Emad, R. Lu, M.-H. Li, Y. Yang, T. Wu, and S. Gong, "Resonant Torsional Micro-Actuators Using Thin-Film Lithium Niobate," in *2019 IEEE 32nd International Conference on Micro Electro Mechanical Systems (MEMS)*, 2019: IEEE, pp. 282-285.

[5] J.-H. Park, J. Akedo, H. J. S. Sato, and A. A. Physical, "High-speed metal-based optical microscanners using stainless-steel substrate and piezoelectric thick films prepared by aerosol deposition method," vol. 135, no. 1, pp. 86-91, 2007.

[6] M. Tani, M. Akamatsu, Y. Yasuda, H. Fujita, and H. Toshiyoshi, "A 2D-optical scanner actuated by PZT film deposited by arc discharged reactive ion-plating (ADRIP) method," in *Proc. IEEE-LEOS Conf. Optical MEMS 2004*, 2004, pp. 188-189.

[7] T. Iseki, M. Okumura, T. J. S. Sugawara, and A. A. Physical, "Shrinking design of a MEMS optical scanner having four torsion beams and arms," vol. 164, no. 1-2, pp. 95-106, 2010.

[8] S. Matsushita, I. Kanno, K. Adachi, R. Yokokawa, and H. J. M. t. Kotera, "Metal-based piezoelectric microelectromechanical systems scanner composed of Pb (Zr, Ti) O 3 thin film on titanium substrate," vol. 18, no. 6, pp. 765-771, 2012.

[9] M. Levy *et al.*, "Fabrication of single-crystal lithium niobate films by crystal ion slicing," vol. 73, no. 16, pp. 2293-2295, 1998.

[10] S. T. Holmström, U. Baran, and H. Urey, "MEMS laser scanners: a review," *Journal of Microelectromechanical Systems,* vol. 23, no. 2, pp. 259-275, 2014.

[11] F. Schrempel, T. Gischkat, H. Hartung, E.-B. Kley, and W. Wesch, "Ion beam enhanced etching of LiNbO3," *Nuclear Instruments and Methods in Physics Research Section B: Beam Interactions with Materials and Atoms,* vol. 250, no. 1-2, pp. 164-168, 2006.

[12] J.-H. Park, J. Akedo, and H. Sato, "High-speed metal-based optical microscanners using stainless-steel substrate and piezoelectric thick films prepared by aerosol deposition method," *Sensors and Actuators A: Physical,* vol. 135, no. 1, pp. 86-91, 2007.

[13] S. Matsushita, I. Kanno, K. Adachi, R. Yokokawa, and H. Kotera, "Metal-based piezoelectric microelectromechanical systems scanner composed of Pb (Zr, Ti) O 3 thin film on titanium substrate," *Microsystem technologies,* vol. 18, no. 6, pp. 765-771, 2012.

[14] F. Filhol, E. Defay, C. Divoux, C. Zinck, and M.-T. Delaye, "Resonant micro-mirror excited by a thin-film piezoelectric actuator for fast optical beam scanning," *Sensors and Actuators A: Physical,* vol. 123, pp. 483-489, 2005.

CONTACT

*Tao Wu, Tel.: +86-21-2068-5357; wutao@ shanghaitech.edu.cn